
Towards truly local gradients with CLAPP: Contrastive, Local And Predictive Plasticity

Bernd Illing

bernd.illing@epfl.ch

Wulfram Gerstner

wulfram.gerstner@epfl.ch

Guillaume Bellec

guillaume.bellec@epfl.ch

Department of Computer Science & Department of Life Sciences
École Polytechnique Fédérale de Lausanne
1015 Switzerland

Abstract

Back-propagation (BP) is costly to implement in hardware and implausible as a learning rule implemented in the brain. However, BP is surprisingly successful in explaining neuronal activity patterns found along the cortical processing stream. We propose a locally implementable, unsupervised learning algorithm, CLAPP, which minimizes a simple, layer-specific loss function, and thus does not need to back-propagate error signals. The weight updates only depend on state variables of the pre- and post-synaptic neurons and a layer-wide third factor. Networks trained with CLAPP build deep hierarchical representations of images and speech.

1 Introduction

Synaptic connection weights in the brain change according to plasticity rules that are ‘local’ and depend only on the recent state of the pre- and post-synaptic neurons [1–3], potentially modulated by a third factor related to surprise or reward [4]. Therefore, one appealing hypothesis is that *representation learning in sensory cortices emerges from local and unsupervised plasticity rules* [5]. However, there seems to be a substantial gap between the rich hierarchical representations observed in the cortex [5] and the representations emerging from such local plasticity rules [6–8]. This is puzzling because learning rules relying on back-propagation (BP) *can* build hierarchical representations similar to those found in visual cortex [9]. Although some progress towards biologically plausible implementations of backpropagation has been made [10–13], it is argued that there are unanswered questions on how the brain could implement some aspects of BP, see e.g. [14].

An important problem of bio-inspired implementations of BP is the dependence of synaptic plasticity on a neuron-specific error signal. Typical implementations require, explicitly or implicitly, that a separate feedback network recalculate and transmit error signals across layers (see Figure 2a). However, ideally no signals other than the activity of neurons inside the main network should be used. Plasticity rules based on contrastive divergence [15] or equilibrium propagation [11] avoid this problem, but the use of stochastic signals [15] or the requirement of complete convergence to equilibrium [11] slows down the algorithms in practical applications.

The present paper makes a step towards demonstrating that rich and deep representation can emerge from a bio-plausible, unsupervised learning rule that is truly local, i.e. only uses variables derived from the momentary state of pre- and post-synaptic neurons and a common third factor that switches

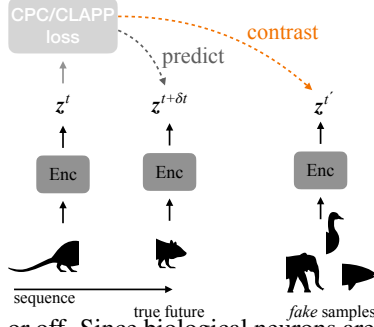


Figure 1: In CPC and CLAPP, an encoder network (Enc) produces a representation z^t at time t (sometimes more generally called ‘context’). Given z^t , the encoding of the future input $z^{t+\delta t}$ should be *predicted* while keeping the prediction as different as possible from encoded *fake* samples $z^{t'}$ (*contrasting*).

plasticity on or off. Since biological neurons are units with a complex dynamical and spatial structure, the momentary state of a neuron is not necessarily compressible into a single ‘activity’ variable, but described by a few variables that may reflect recent input into different parts of the neuronal dendrites. Our approach takes inspiration from deep unsupervised learning algorithms that seek to contrast, cluster or predict stimuli in the context of BP [16–19]. We build upon this body of work and suggest the *Contrastive, Local And Predictive Plasticity* (CLAPP) model which avoids BP completely.

CLAPP handles time-varying inputs (as demonstrated later on the LibriSpeech dataset). In recurrent networks, the representation learning with CLAPP can be further combined with e-prop [20], resulting in an algorithm that avoids both, BP through time and network depth. Independently of its relation to neuroscience, we believe that CLAPP is also attractive for computing hardware. We expect that CLAPP reduces the memory load on GPUs [19] compared to training with BP. Furthermore, current neuromorphic hardware favors local learning rules [21–23].

2 Background and State-of-the-Art

Contrastive predictive coding (CPC) The CPC algorithm [16] trains an *encoder* (for example a deep neural network) to predict its responses to future inputs while contrasting against its responses to *fake* inputs, called negative samples (see Figure 1). The encoder representation z^t – also referred to as the *context* in [16] – makes a prediction $\mathbf{W}^{\text{pred}} z^t$ of the encoding $z^{t+\delta t}$ at time $t + \delta t$. The learning objective is implemented as a classification problem: given the prediction, the task is to distinguish the representation of true future $z^{t+\delta t}$ from that of negative examples $z^{t'}$, sampled uniformly at arbitrary time points (t' may come from the same or a different input sequence). Mathematically this is formalized by the loss function $\mathcal{L}_{\text{CPC}}^t$ and a score function u_t^τ defined as:

$$\mathcal{L}_{\text{CPC}}^t = -\log \frac{\exp u_t^{t+\delta t}}{\sum_{\tau \in \mathcal{T}} \exp u_t^\tau}, \quad \text{with} \quad u_t^\tau = z^{\tau \top} \mathbf{W}^{\text{pred}} z^t, \quad (1)$$

where the elements of the matrix \mathbf{W}^{pred} are learned model parameters and $\mathcal{T} = \{t^{t+\delta t}, t'_1 \dots t'_N\}$ comprises the positive and N negative samples. The loss function is minimized by BP [16]. A recurring problem when modelling learning in the brain with BP-like algorithms is that a layer l has to transmit complex error signals to layer $l - 1$, i.e. information other than its own neural activity. This typically requires the existence of an auxiliary feedback network [14, 24] (see Figure 2a).

Greedy InfoMax (GIM) is a variant of CPC where the deep encoder network is split into a few modules. Each module is composed of several layers and has its own loss function. The back-propagated gradients are then blocked between these modules (see Figure 4) [19]. In the extreme case when each gradient-isolated module contains a single layer (*layer-wise GIM*) the performance is partially compromised (see section 4 or [25]) but the learning algorithm becomes almost BP-free. This is a first step towards local learning rules, but the gradients of the layer-specific CPC losses (equation 1) require complex computations that remain implausible (see Appendix A for details).

3 Gradient of a contrastive and predictive loss is a local learning rule

Hinge Loss CPC. The gradient computation in layer-wise GIM raises at least two problems that we analyse in Appendix A. First, it requires the transmission of information other than the network activity. Second, the gradient computation requires computing weighing factors (or probabilities) $\frac{1}{\sum \exp u_t^\tau}$ which combine the scores u_t^τ of positive and negative samples in a non-linear way. It is not clear how these computations could be implemented by neurons in real brains.

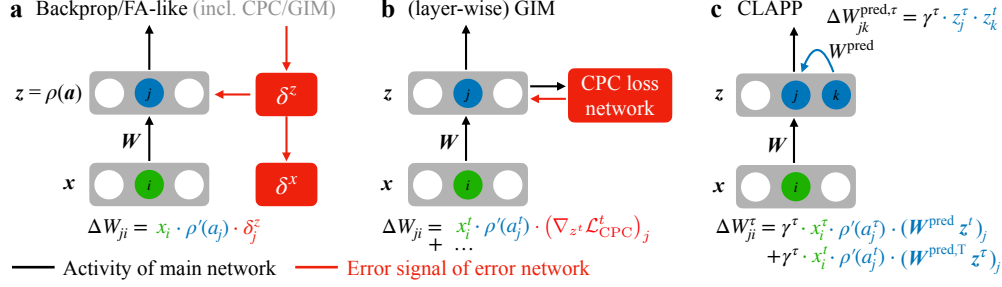


Figure 2: Weight update computation for networks trained with **a** backpropagation (BP), **b** layer-wise Greedy InfoMax (GIM) and **c** our Contrastive Local and Predictive Plasticity (CLAPP). BP and feedback alignment (FA) -like methods require separate error networks for computing and transmitting error signals. Layer-wise GIM does not transmit error signals but still needs a separate network per layer to compute updates. CLAPP calculates updates purely based on neural activity within the layer using recurrent connections \mathbf{W}^{pred} .

Here, we start from GIM but suggest a simpler loss function for which gradient descent gives rise to a plausible model of synaptic plasticity. This alternative differs from \mathcal{L}_{CPC}^t in two ways: (1) we perform binary comparisons between positive $z^{t+\delta t}$ and negative samples $z^{t'}$ instead of comparing a group of negative samples simultaneously, and (2) this binary classification is implemented with the Hinge loss instead of cross-entropy. We call this the *Contrastive Local And Predictive Plasticity* (CLAPP) loss and define it as $\mathcal{L}_{CLAPP}^t = \mathcal{L}_{CLAPP}^{t, \text{pos}} + \mathcal{L}_{CLAPP}^{t, \text{neg}}$ with

$$\mathcal{L}_{CLAPP}^{t, \text{pos}} = \begin{cases} 1 - u_t^{t+\delta t} & \text{if } u_t^{t+\delta t} < 1 \\ 0 & \text{otherwise,} \end{cases} \quad \text{and} \quad \mathcal{L}_{CLAPP}^{t, \text{neg}} = \begin{cases} 1 + u_t^{t'} & \text{if } u_t^{t'} > -1 \\ 0 & \text{otherwise.} \end{cases} \quad (2)$$

A first advantage of this loss function is that it is linearly additive. The contributions of different samples are simply added up instead of being combined non-linearly as in \mathcal{L}_{CPC} . Hence, updates stemming from positive and negative samples can be processed in arbitrary order or at different times (modelling potentially that inference happens during the day and dreaming happens at night).

A second advantage is that the loss function is piece-wise linear in the score function u_t^τ (see Figure 5), and u_t^τ in turn is linear in z^t , z^τ and \mathbf{W}^{pred} , which leads to a remarkably simple weight update. For instance an online gradient descent update with learning rate η for the parameter \mathbf{W}^{pred} results in a gated Hebbian plasticity rule. Using a global factor $\gamma^\tau = 0$ when the loss for prediction τ vanishes and $\gamma^\tau = \eta$ when the score u_t^τ has to increase for a positive sample, or decrease for a negative sample, we have

$$\Delta W_{jk}^{\text{pred}} = \Delta W_{jk}^{\text{pred}, t+\delta t} - \Delta W_{jk}^{\text{pred}, t'}, \quad \text{with} \quad \Delta W_{jk}^{\text{pred}, \tau} = \gamma^\tau z_j^\tau z_k^t, \quad (3)$$

where k and j denote the pre- and post-synaptic neurons in layer z . We see that positive ($\tau = t + \delta t$) and negative (t') samples contribute similarly but with opposite sign. Perhaps more interestingly, the update of the parameters involved in the feedforward processing of the input leads to a Hebbian rule, modulated by the recurrent activity of other neurons. Let us write the activity of layer z as $z^t = \rho(a^t)$ with $a^t = \mathbf{W}x^t$, where x^t is the input and $\rho(\cdot)$ the nonlinearity of layer z (we absorb the bias b into \mathbf{W}). For the update of \mathbf{W} we find $\Delta W_{ji} = \Delta W_{ji}^{t+\delta t} - \Delta W_{ji}^{t'}$ with

$$\Delta W_{ji}^\tau = \gamma^\tau \left[(\mathbf{W}^{\text{pred}} z^t)_j \rho'(a_j^\tau) x_i^\tau + (\mathbf{W}^{\text{pred}, \top} z^\tau)_j \rho'(a_j^t) x_i^t \right], \quad (4)$$

where i denotes a pre-synaptic neuron in layer x below z in the network hierarchy and j denotes a post-synaptic neuron in layer z . Therefore, the plasticity of \mathbf{W} takes the form of a three factor learning rule where the third factor is the common factor γ^τ and the postsynaptic factor is a combination of two parts, i.e., the derivative ρ' and a *linear projection of the activity* of other neurons in the same layer, e.g., summarizing the input into one part of the dendrite of neuron j .

Since almost all the information transmission takes the form of neural activity, the plasticity rule solves many plausibility issues of BP described in [14]. The gating factor γ^τ acts globally and requires a simpler mechanism than a neuron specific feedback pathway and is reminiscent of traditional models of neuromodulators [4]. The update $\Delta \mathbf{W}$ requires weight transport since \mathbf{W}^{pred} and $\mathbf{W}^{\text{pred}, \top}$ take part in equation (4) but we can solve this easily by introducing two independent \mathbf{W}^{pred} s as detailed in Appendix C. To yield a learning rule that is also plausible with recurrent networks, we combine e-prop [20] with CLAPP as explained in Appendix C.

Table 1: Linear classification test accuracy [%] on STL-10 and phone classification on LibriSpeech (LS). Features for classification come from the encoder trained with different methods. CLAPP performs best among methods not using error backpropagation in the encoder (BP-free). For LS, BP through time is used. Values with * are taken from Löwe et al. [19]. For details, see Appendix B.

Method	BP-free?	STL-10	LS
Random ini.	✓	21.8	27.7*
MFCC	✓	-	39.7*
Greedy supervised	✓	65.0	73.4*
Supervised		73.2	77.7*
CPC		81.1	64.3
GIM (as in [19])		78.3	63.9
Hinge Loss CPC (ours)		80.3	62.8
CLAPP (ours)	✓	74.0	61.7

4 Empirical Results

As in Löwe et al. [19], we evaluate the CLAPP model on the image and audio processing tasks from the STL-10 [26] and LibriSpeech [27], datasets (see Appendix B). For vision experiments we replace the ResNet-50 encoder used in [19] by a 6 layer VGG-like encoder (VGG-6) - without compromising downstream performance (see Appendix B). In all experiments we first train the encoder without supervision and freeze its weights, then, we evaluate the quality of the encoded representations using the accuracy of a linear classification of the image labels.

We see in Table 1 that CLAPP outperforms other backpropagation-free methods by almost 10 % on STL-10. Furthermore it beats supervised training, implying that it leverages the large unlabeled dataset. In phone classification CLAPP even approaches the performance of end-to-end CPC. To understand the remaining performance gap between CPC and CLAPP we empirically investigate the two simplification steps that led from CPC to CLAPP: *i*) Simplifying the CPC loss function itself and *ii*) reducing the loss function to local, layer-wise computations.

Simplifying CPC. To study the effect of loss simplification, we first train the encoder end-to-end and simplify the loss function from \mathcal{L}_{CPC}^t to \mathcal{L}_{CLAPP}^t . We found that a binary comparison between the positive and one negative sample (using a Binary Cross-Entropy loss) only marginally reduces downstream performance (80.6 % test acc.) compared to CPC (81.1 %). Changing from binary cross-entropy to the piece-wise linear CLAPP loss (Equation 2) also leaves performance almost untouched (Hinge Loss CPC, 80.3 %).

Layer-wise losses. In the second step from GIM to CLAPP, we restrict the number of layers per gradient-isolated module to one. Figure 3 shows that the depth of the encoder is still exploited and that CLAPP *builds deep hierarchical representations*: classifying from higher encoder layers leads to higher performance (i.e. it is *stackable*). Furthermore, the difference in performance between end-to-end CPC and CLAPP is almost the same as between CPC and (layer-wise) GIM, confirming that CLAPP does not suffer from the other simplifications of the loss function in the layer-wise setting. In the inset of Figure 3 we give an intuition of the effect of gradient blocking within the encoder: we perform a series of experiments with one gradient-isolated module encoder (Hinge Loss CPC) up to 6 modules (CLAPP). Interestingly, the modest decrease in performance is monotonic with the number of modules, yet stays competitive even in the case of 6 modules, i.e. fully local, layer-wise training.

5 Discussion

We introduced CLAPP, a locally implementable, unsupervised learning algorithm that can build deep hierarchical representations in neural networks. It yields a biologically plausible model of synaptic plasticity supporting competitive unsupervised deep learning. Currently, CLAPP requires perfect recall of negative samples $\mathbf{z}^{t'}$, and the recurrent activity $\mathbf{W}^{\text{pred}} \mathbf{z}^t$ does not take part in the inference. So far, we did not cover these two aspects of the model’s plausibility and keep them for future work.

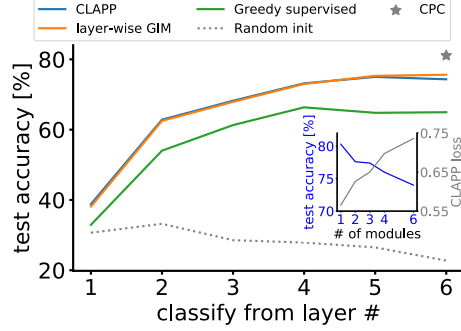


Figure 3: **Main:** Every layer of the encoder extracts more useful representations for the linear downstream classification on STL-10, despite the lack of top-down gradients. **Inset:** Performance degrades gracefully with the number of gradient-isolated modules in the VGG-6 encoder (at fixed number of encoder layers).

Acknowledgments and Disclosure of Funding

This research was supported by the Swiss National Science Foundation (no. 200020_184615) and by the European Union Horizon 2020 Framework Program under grant agreement no. 785907 (Human Brain Project, SGA2).

References

- [1] Per Jesper Sjöström, Gina G Turrigiano, and Sacha B Nelson. Rate, timing, and cooperativity jointly determine cortical synaptic plasticity. *Neuron*, 32(6):1149–1164, 2001.
- [2] Natalia Caporale and Yang Dan. Spike timing–dependent plasticity: a hebbian learning rule. *Annu. Rev. Neurosci.*, 31:25–46, 2008.
- [3] Claudia Clopath, Lars Büsing, Eleni Vasilaki, and Wulfram Gerstner. Connectivity reflects coding: a model of voltage-based stdp with homeostasis. *Nature neuroscience*, 13(3):344, 2010.
- [4] Wulfram Gerstner, Marco Lehmann, Vasiliki Liakoni, Dane Corneil, and Johanni Brea. Eligibility traces and plasticity on behavioral time scales: experimental support of neohebbian three-factor learning rules. *Frontiers in neural circuits*, 12:53, 2018.
- [5] James J DiCarlo, Davide Zoccolan, and Nicole C Rust. How does the brain solve visual object recognition? *Neuron*, 73(3):415–434, 2012.
- [6] Christopher J Rozell, Don H Johnson, Richard G Baraniuk, and Bruno A Olshausen. Sparse coding via thresholding and local competition in neural circuits. *Neural computation*, 20(10):2526–2563, 2008.
- [7] Teuvo Kohonen. *Self-organizing maps*, volume 30. Springer Science & Business Media, 2012.
- [8] Cengiz Pehlevan, Anirvan M Sengupta, and Dmitri B Chklovskii. Why do similarity matching objectives lead to hebbian/anti-hebbian networks? *Neural computation*, 30(1):84–124, 2018.
- [9] Daniel LK Yamins, Ha Hong, Charles F Cadieu, Ethan A Solomon, Darren Seibert, and James J DiCarlo. Performance-optimized hierarchical models predict neural responses in higher visual cortex. *Proceedings of the National Academy of Sciences*, 111(23):8619–8624, 2014.
- [10] Timothy P Lillicrap, Daniel Cownden, Douglas B Tweed, and Colin J Akerman. Random synaptic feedback weights support error backpropagation for deep learning. *Nature communications*, 7(1):1–10, 2016.
- [11] Benjamin Scellier and Yoshua Bengio. Equilibrium propagation: Bridging the gap between energy-based models and backpropagation. *Frontiers in computational neuroscience*, 11:24, 2017.
- [12] Alexandre Payeur, Jordan Guerguiev, Friedemann Zenke, Blake Richards, and Richard Naud. Burst-dependent synaptic plasticity can coordinate learning in hierarchical circuits. *bioRxiv*, 2020.
- [13] João Sacramento, Rui Ponte Costa, Yoshua Bengio, and Walter Senn. Dendritic cortical microcircuits approximate the backpropagation algorithm. In *Advances in neural information processing systems*, pages 8721–8732, 2018.
- [14] Timothy P. Lillicrap, Adam Santoro, Luke Marris, Colin J. Akerman, and Geoffrey Hinton. Backpropagation and the brain. *Nat. Rev. Neurosci.*, 21(6):335–346, 2020. ISSN 14710048. doi: 10.1038/s41583-020-0277-3.
- [15] Geoffrey E Hinton. Training products of experts by minimizing contrastive divergence. *Neural computation*, 14(8):1771–1800, 2002.
- [16] Aaron van den Oord, Yazhe Li, and Oriol Vinyals. Representation Learning with Contrastive Predictive Coding. *arXiv Prepr.*, 2018.

- [17] Mathilde Caron, Piotr Bojanowski, Armand Joulin, and Matthijs Douze. Deep clustering for unsupervised learning of visual features. In *Proceedings of the European Conference on Computer Vision (ECCV)*, pages 132–149, 2018.
- [18] Chengxu Zhuang, Alex Lin Zhai, and Daniel Yamins. Local aggregation for unsupervised learning of visual embeddings. In *Proceedings of the IEEE International Conference on Computer Vision*, pages 6002–6012, 2019.
- [19] Sindy Löwe, Peter O’Connor, and Bastiaan S. Veeling. Putting An End to End-to-End: Gradient-Isolated Learning of Representations. *Advances in neural information processing systems*, 2019.
- [20] Guillaume Bellec, Franz Scherr, Anand Subramoney, Elias Hajek, Darjan Salaj, Robert Legenstein, and Wolfgang Maass. A solution to the learning dilemma for recurrent networks. *Nature communications*, 11, 2020.
- [21] Steve B Furber, Francesco Galluppi, Steve Temple, and Luis A Plana. The spinnaker project. *Proceedings of the IEEE*, 102(5):652–665, 2014.
- [22] Mike Davies, Narayan Srinivasa, Tsung-Han Lin, Gautham Chinya, Yongqiang Cao, Sri Harsha Choday, Georgios Dimou, Prasad Joshi, Nabil Imam, Shweta Jain, et al. Loihi: A neuromorphic manycore processor with on-chip learning. *IEEE Micro*, 38(1):82–99, 2018.
- [23] Timo Wunderlich, Akos F Kungl, Eric Müller, Andreas Hartel, Yannik Stradmann, Syed Ahmed Aamir, Andreas Grübl, Arthur Heimbrecht, Korbinian Schreiber, David Stöckel, et al. Demonstrating advantages of neuromorphic computation: a pilot study. *Frontiers in neuroscience*, 13: 260, 2019.
- [24] Isabella Pozzi, Sander M Bohté, and Pieter R Roelfsema. A Biologically Plausible Learning Rule For Deep Learning In The Brain. *arXiv Prepr.*, pages 1–14, 2018.
- [25] Yuwen Xiong, Mengye Ren, and Raquel Urtasun. LoCo: Local Contrastive Representation Learning. *Advances in neural information processing systems*, 2020.
- [26] Adam Coates, Andrew Ng, and Honglak Lee. An analysis of single-layer networks in unsupervised feature learning. In *Proceedings of the fourteenth international conference on artificial intelligence and statistics*, pages 215–223, 2011.
- [27] Vassil Panayotov, Guoguo Chen, Daniel Povey, and Sanjeev Khudanpur. Librispeech: an asr corpus based on public domain audio books. In *2015 IEEE International Conference on Acoustics, Speech and Signal Processing (ICASSP)*, pages 5206–5210. IEEE, 2015.
- [28] Adam Paszke, Sam Gross, Soumith Chintala, Gregory Chanan, Edward Yang, Zachary DeVito, Zeming Lin, Alban Desmaison, Luca Antiga, and Adam Lerer. Automatic differentiation in pytorch. 2017.
- [29] Arild Nøkland and Lars Hiller Eidnes. Training Neural Networks with Local Error Signals. *International Conference on Machine Learning*, 2019. doi: arXiv:1901.06656v1.

Supplemental material for:

Towards truly local gradients with CLAPP: Contrastive, Local And Predictive Plasticity

Notation in supplementary sections In all supplementary sections, and in line with [16, 19], the context vector, from which the prediction is performed, is denoted \mathbf{c}^t and the feature vector being predicted is denoted $\mathbf{z}^{t+\delta t}$ (or $\mathbf{z}^{t'}$ for negative samples). In general, the loss function of CPC and CLAPP are therefore defined with the score functions $u_t^\tau = \mathbf{z}^{\tau\top} \mathbf{W}^{\text{pred}} \mathbf{c}^t$.

Throughout the vision experiments and when training the temporal convolutions of the audio processing network, it happens that \mathbf{c} and \mathbf{z} denote the same layer (see Appendix B for details). However, when processing audio, the highest loss uses the last layer as the context layer \mathbf{c} and the one before last for \mathbf{z} .

To cover the most general case, we introduce different notations for the parameters and the variables of the context layer \mathbf{c} and the feature layer \mathbf{z} . For simplicity our analysis considers standard, fully-connected networks – even if the reasoning generalises easily to other architectures. Hence, with a non-linearity ρ , the feature layer produces the activity $\mathbf{z}^t = \rho(\mathbf{a}^{\mathbf{z},t})$ with $\mathbf{a}^{\mathbf{z},t} = \mathbf{W}^{\mathbf{z}} \mathbf{x}^{\mathbf{z},t} + \mathbf{b}^{\mathbf{z}}$ where $\mathbf{x}^{\mathbf{z},t}$, $\mathbf{W}^{\mathbf{z}}$ and $\mathbf{b}^{\mathbf{z}}$ are the input vector (at time t), weight matrix and bias respectively (the layer index l is omitted for simplicity). The notation naturally extends to the context layer \mathbf{c} and we use $\mathbf{x}^{\mathbf{c},t}$, $\mathbf{W}^{\mathbf{c}}$ and $\mathbf{b}^{\mathbf{c}}$ to denote its input and its parameters. Note that in the main text, context and feature layer are the same layer \mathbf{z} and thus the two parameters $\mathbf{W}^{\mathbf{c}}$ and $\mathbf{W}^{\mathbf{z}}$ are actually only one single parameter \mathbf{W} and the weight update is given by $\Delta \mathbf{W} = \Delta \mathbf{W}^{\mathbf{c}} + \Delta \mathbf{W}^{\mathbf{z}}$.

For the gradient computations in the supplementary sections we assume that the gradient cannot propagate further than one layer. Hence, $\mathbf{x}^{\mathbf{z}}$ and $\mathbf{x}^{\mathbf{c}}$ are always considered as constants with respect to all parameters even though this is technically not true when the input of layer \mathbf{c} is \mathbf{z} . In this case we would have $\mathbf{z} = \mathbf{x}^{\mathbf{c}}$ and thus $\nabla_{\mathbf{W}^{\mathbf{z}}} \mathbf{x}^{\mathbf{c}} \neq \mathbf{0}$, but we use the convention $\nabla_{\mathbf{W}^{\mathbf{z}}} \mathbf{x}^{\mathbf{c}} = \mathbf{0}$ to obtain local learning rules. Gradients are computed accordingly by stopping gradient propagation in our experiments.

A Analysis of the original CPC gradient

Even after preventing gradients to flow from a layer to the next, we argue that parts of the gradient computation in CPC and GIM are hard to implement with the type of information processing that is possible in neural circuits. For this reason we analyse the actual gradients computed by layer-wise GIM. We further discuss the bio-plausibility of the resulting gradient computation in this section.

To derive the loss gradient we define the probability π_t^{t*} that the sample \mathbf{z}^{t*} is predicted as the true future given the context layer \mathbf{c}^t : $\pi_t^{t*} \stackrel{\text{def}}{=} \frac{1}{Z} \exp u_t^{t*}$ with $Z \stackrel{\text{def}}{=} \sum_{\tau \in \mathcal{T}} \exp u_t^\tau$. The set $\mathcal{T} = \{t^{t+\delta t}, t'_1 \dots t'_N\}$ comprises the positive and N negative samples. We have in particular $\mathcal{L}_{CPC}^t = -\log \pi_t^{t+\delta t}$ and for any parameter θ the (negative) loss gradient is given by:

$$\nabla_\theta \log \pi_t^{t+\delta t} = \nabla_\theta u_t^{t+\delta t} - \sum_{\tau \in \mathcal{T}} \pi_t^\tau \nabla_\theta u_t^\tau. \quad (5)$$

We consider only three types of parameters: the weights $\mathbf{W}^{\mathbf{c}}$ onto the context vector \mathbf{c}^t , the weights $\mathbf{W}^{\mathbf{z}}$ onto the feature vector \mathbf{z}^{t*} and the weights \mathbf{W}^{pred} defining the scalar score $u_t^{t*} = \mathbf{z}^{t*\top} \mathbf{W}^{\text{pred}} \mathbf{c}^t$ (the biases are absorbed in the weight matrices for simplicity).

Let's first analyze the gradient with respect to \mathbf{W}^{pred} . Using the conventions that k is the index of the context unit c_k and j is the index of the feature unit z_j , we have:

$$\nabla_{W_{jk}^{\text{pred}}} \log \pi_t^{t+\delta t} = c_k^t \left(z_j^{t+\delta t} - \sum_{\tau \in \mathcal{T}} \pi_t^\tau z_j^\tau \right) \quad (6)$$

Viewing a gradient descent weight update of that parameter as a model of synaptic plasticity in the brain raises essential questions. If $z_j^{t+\delta t} - \sum_{\tau \in \mathcal{T}} \pi_t^\tau z_j^\tau$ was the activity of the unit j , it would boil down to a Hebbian learning rule, well supported experimentally, but the activity of unit j is considered to be the vector element z_j since it is transmitted to the layer above during inference. Hence, the unit j would have to transmit two distinct quantities at the same time, which is unrealistic when modelling real neurons. On top of that, it is unclear how the term $\sum_{\tau \in \mathcal{T}} \pi_t^\tau z_j^\tau$ would be computed.

We now compute the gradient with respect to W^c and W^z . The update of these parameters raises an extra complication because it involves the activity of more than two units. For the parameters of the layer z we denote j a neuron in this layer, and i a neuron from its input layer x . Then the loss gradient is given by:

$$\nabla_{W_{ji}^z} \log \pi_t^{t+\delta t} = (W^{\text{pred}} c^t)_j \left(\rho'(a_j^z)^{t+\delta t} x_i^{z,t+\delta t} - \sum_{\tau \in \mathcal{T}} \pi_t^\tau \rho'(a_j^z)^\tau x_i^{z,\tau} \right). \quad (7)$$

Similarly, for the parameters of a neuron c_j^t :

$$\nabla_{W_{ji}^c} \log \pi_t^{t+\delta t} = \left(W^{\text{pred}, \top} \left(z^{t+\delta t} - \sum_{\tau \in \mathcal{T}} \pi_t^\tau z^\tau \right) \right)_j \rho'(a_j^c)^t x_i^{c,t}. \quad (8)$$

These gradients raise the same essential problems as the computation of the gradients with respect to W^{pred} and even involve other complex computations.

B Simulation details

We use pytorch [28] for our implementation and base it on the code base of the GIM paper [19]¹. Unless mentioned otherwise we adopt their setup, data sets, data handling and (hyper-)parameters.

B.1 Vision experiments

General procedure The encoder network is trained with either CPC, GIM or CLAPP on unlabeled data. Since CPC-like methods rely on sequences of data we have to introduce an artificial ‘temporal’ dimension in the case of vision data sets. This is done by splitting the image into partially overlapping tiles or patches. The encoder is then applied to patches located in the upper half of the image and CPC is applied to predict/contrast encodings of lower patches in the image. The hyperparameters of this procedure and of other image preprocessing steps are unchanged to the ones in Löwe et al. [19].

We then freeze the encoder network and train a linear downstream classifier on representations created by the encoder using held-out, labeled data. The accuracy of that classification serves as a measure to evaluate the quality of the learned encoder representations.

Encoder architecture We use VGG-6, a custom 6-layer VGG-like encoder (see Table 2). The architecture choice was inspired by the condensed VGG-like architectures successfully applied in Nøkland and Eidnes [29]. The main motivation was to work with an architecture that allows pure layer-wise training which is impossible in e.g. ResNet-50 due to skip-connections. Surprisingly we find that the transition from ResNet-50 to VGG-6 does neither compromise CPC losses nor downstream classification performance for almost all training methods, see Table 4.

In GIM and CLAPP, the encoder is split into several, gradient-isolated modules. Depending on the number of such modules, each module contains a different number of layers. In CPC we do not use any gradient blocking and consequently the encoder consists only of one module containing layers 1-6. In layer-wise GIM and CLAPP each of the 6 modules contains exactly one layer (and potentially another MaxPooling layer). Table 3 shows the distribution of layers into modules for the cases in between.

¹https://github.com/loeweX/Greedy_InfoMax

# of trainable layer	layer type
1	3×3 conv128, ReLU
2	3×3 conv256, ReLU 2×2 MaxPool
3	3×3 conv256, ReLU
4	3×3 conv512, ReLU 2×2 MaxPool
5	3×3 conv1024, ReLU 2×2 MaxPool
6	3×3 conv1024, ReLU 2×2 MaxPool

Table 2: Architecture of the VGG-6 encoder network. Convolutional layers (conv) have stride (1, 1), Pooling layers use stride (2, 2). The architecture is inspired by the VGG-like networks used in Nøkland and Eidnes [29].

# of modules	layer distribution
1 (CPC)	(1,2,3,4,5,6)
2	(1,2,3), (4,5,6)
3	(1,2), (3,4), (5,6)
4	(1,2,3),(4),(5),(6) or (1),(2),(3),(4,5,6)
6	(1),(2),(3),(4),(5),(6)

Table 3: Distribution of layers into modules as done for the simulations in the inset of Table 3 and Table 5. The layer numbers refer to Table 2.

Reference algorithms *Random init* refers to the random initialisation of the encoder network. It thus represents an untrained network with random weight matrices. This ‘method’ serves as a lower bound on performance and as a sanity check for other algorithms.

In classic *supervised* training, we add a fully-connected layer with as many output dimensions as classes in the data set to the encoder architecture. Then the whole stack is trained end-to-end using a standard supervised loss and back-propagation. For data sets offering many labels this serves as an upper bound on performance of unsupervised methods. In the case of sparsely labeled data, unsupervised learners could, or even should, outperform supervised learning.

Greedy supervised training trains every gradient-isolated module of the encoder separately. For that, we add a fully-connected layer to each module. Then, for every module, the stack consisting of the module and the added fully-connected layer is trained with a standard supervised loss and back-propagation within the module.

B.2 Audio experiments

We follow most of the implementation methods used in [19]. The model is trained without supervision on 100 hours of clean spoken sentences from the LibriSpeech data set and we did not apply data augmentation. To test the emergence of rich latent features, a linear classifier is used to extract the phonemes. This classifier is trained on the test split of the same dataset, along with the phoneme annotations computed with a software in [16].

The audio stream is first processed with four 1D convolutional layers and one recurrent layer of Gated Recurrent Units (GRU). The hyperparameters of this architecture are the same as the ones used in Löwe et al. [19].

All convolutional layers are assigned a CPC or a CLAPP loss as described in the main text and the gradients are blocked between them. To train the last layer – the recurrent layer –, we add one variant of the CLAPP and CPC losses where the score function is defined by $u_t^\tau = \mathbf{z}^{\tau^\top} \mathbf{W}^{\text{pred}} \mathbf{c}^t$ where \mathbf{c}^t is the activity of the GRU layer and \mathbf{z}^τ is the activity of the last layer of convolutions. This loss

Table 4: Linear classification test accuracy (%) on STL-10 with features coming from two different encoder models: ResNet-50 as in Löwe et al. [19] and a 6-layer VGG-like encoder (VGG-6). Values for ResNet-50 are taken from Löwe et al. [19].

	ResNet-50	VGG-6
Random init	27.0	21.8
Greedy Supervised	65.2	65.0
Supervised	71.4	73.2
CPC	80.5	81.1
GIM (3 modules)	81.9	78.3

is minimized with respect to the parameters of c and z , and the gradients cannot flow to the layers below (hence $\nabla_{Wz} c^t = 0$ even if z is implicitly the input to c with this architecture).

Within the GRU layer the usual implementation of gradient descent with pytorch involves back-propagation through time (BPTT), even if we avoided BP between layers. To avoid all usage of back-propagation and obtain a more plausible learning rule we used e-prop [20] instead of BPTT. The details of this implementation are provided in the next section (Appendix C) in the paragraph “Combining e-prop and CLAPP”.

C Additional material

Weight transport in W^{pred} CLAPP relies on weight transport in Equation 4 since the activity of z^t is propagated with the matrix W^{pred} and z^τ with its transpose. This is problematic because typical synapses in the brain transmit information only in a single direction. The existence of a symmetric reverse connection matrix would solve this problem but raises the issue that connection strengths would have to be synchronised (hence the word *weight transport*) between W^{pred} and the reverse connections.

One first naive solution is to block the gradient at the layer c in the definition of the score $u_t^\tau = z^{\tau \top} W^{\text{pred}} \text{block_grad}(c^t)$, with the definition:

$$\begin{aligned} \text{block_grad}(x) &= x \\ \nabla_x \text{block_grad}(x) &= 0. \end{aligned} \quad (9)$$

In this way, no information needs to be transmitted through the transpose of W^{pred} . However this results in a relatively large drop in performance on STL-10 for Hinge Loss CPC (78.0 %) and CLAPP (70 %).

A better option is to split W^{pred} into two matrices W_z^{pred} and W_c^{pred} which are independent and which allow information flow only in a single direction (as in actual biological synapses). To this end, we split the loss function into two parts: one part receives the activity $W_z^{\text{pred}} c^t$ coming from c^t and only updates the parameters of z ; and the other part receives the activity $W_c^{\text{pred}} z^\tau$ coming from z^τ and updates the parameters of c . As we see in the following paragraph, this modifies the weight update from Equation 4 such that it requires transmitting information through W_c^{pred} and W_z^{pred} instead of W^{pred} and its transpose matrix and hence solves the weight transport problem.

More formally, let us write F to summarize the definition of the usual CLAPP loss function in Equation 2 such that $\mathcal{L}_{\text{CLAPP}}^t = F(c^t, z^\tau, W^{\text{pred}})$. We then introduce a modified version of the CLAPP loss function:

$$\tilde{\mathcal{L}}_{\text{CLAPP}}^t = \frac{1}{2} \left(\tilde{\mathcal{L}}_{\text{CLAPP}}^{t,c} + \tilde{\mathcal{L}}_{\text{CLAPP}}^{t,z} \right), \quad (10)$$

with $\tilde{\mathcal{L}}_{\text{CLAPP}}^{t,z} = F(\text{block_grad}(c^t), z^\tau, W_z^{\text{pred}})$ and $\tilde{\mathcal{L}}_{\text{CLAPP}}^{t,c} = F(c^t, \text{block_grad}(z^\tau), W_c^{\text{pred}})$. Similarly, we define the corresponding scores as $u_t^{\tau,z} = z^{\tau \top} W_z^{\text{pred}} \text{block_grad}(c^t)$ and $u_t^{\tau,c} = \text{block_grad}(z^\tau)^\top W_c^{\text{pred}} c^t$. With this, the gradients with respect to the weight parameters W_{ji}^z are:

$$\frac{\partial u_t^{\tau,z}}{\partial W_{ji}^z} = x_i^{\tau,z} \rho'(a_j^{\tau,z}) (W_z^{\text{pred}} c^t)_j \quad \text{and} \quad \frac{\partial u_t^{\tau,c}}{\partial W_{ji}^z} = 0, \quad (11)$$

and the gradients with respect to the weights W_{ji}^c become:

$$\frac{\partial u_t^{\tau,z}}{\partial W_{ji}^c} = 0 \quad \text{and} \quad \frac{\partial u_t^{\tau,c}}{\partial W_{ji}^c} = x_i^{t,c} \rho'(a_j^{t,c}) (\mathbf{W}_c^{\text{pred}} \mathbf{z}^\tau)_j. \quad (12)$$

The final plasticity rule that replaces Equation 4 combines those terms with the same gating factor γ^τ as previously (the gating factor does not change since $u_t^\tau = u_t^{\tau,c} = u_t^{\tau,z}$, only their gradients are different):

$$\Delta W_{ji}^{\tau,z} = \gamma^\tau (\mathbf{W}_z^{\text{pred}} \mathbf{c}^t)_j \rho'(a_j^{\tau,z}) x_i^{\tau,z} \quad (13)$$

$$\Delta W_{ji}^{\tau,c} = \gamma^\tau (\mathbf{W}_c^{\text{pred}} \mathbf{z}^\tau)_j \rho'(a_j^{t,c}) x_i^{t,c}, \quad (14)$$

and we see that the propagation of the activity through the independent weights $\mathbf{W}_z^{\text{pred}}$ and $\mathbf{W}_c^{\text{pred}}$ is always unidirectional. It turns out that, using the modified loss $\tilde{\mathcal{L}}_{\text{CLAPP}}^t$, Equation 10, instead of the original CLAPP loss $\mathcal{L}_{\text{CLAPP}}^t$, Equation 2, the performance on STL-10 is unchanged for Hinge Loss CPC (80.2 %) and CLAPP (74.1 %).

Combining e-prop and CLAPP CLAPP avoids the usage of back-propagation through the depth of the network, but when using a recurrent GRU layer in the audio task, gradients are still back-propagated through time inside the layer. A more plausible alternative algorithm has been suggested in Bellec et al. [20]: synaptic eligibility traces compute local gradients forward in time using the activity of pre- and post-synaptic units, then these traces are merged with the learning signal (here $\mathbf{W} \mathbf{z}^{t+\delta t}$) to form the weight update. It is simple to implement e-prop with an auto-differentiation software such as pytorch by introducing a `block_grad` function in the update of the recurrent network. With GRU, we implement a custom recurrent network as follows (the notations are consistent with the pytorch tutorial on GRU networks² and unrelated to the rest of the paper):

$$\mathbf{r}_t = \sigma(\mathbf{W}_{ir} \mathbf{x}_t + \mathbf{b}_{ir} + \mathbf{W}_{hr} \text{block_grad}(\mathbf{h}_{t-1}) + \mathbf{b}_{hr}) \quad (15)$$

$$\mathbf{z}_t = \sigma(\mathbf{W}_{iz} \mathbf{x}_t + \mathbf{b}_{iz} + \mathbf{W}_{hz} \text{block_grad}(\mathbf{h}_{t-1}) + \mathbf{b}_{hz}) \quad (16)$$

$$\mathbf{n}_t = \tanh(\mathbf{W}_{in} \mathbf{x}_t + \mathbf{b}_{in} + \mathbf{r}_t \star (\mathbf{W}_{hn} \text{block_grad}(\mathbf{h}_{t-1}) + \mathbf{b}_{hn})) \quad (17)$$

$$\mathbf{h}_t = (1 - \mathbf{z}_t) \star \mathbf{n}_t + \mathbf{z}_t \star \mathbf{h}_{t-1} \quad (18)$$

In summary we use \mathbf{h}_t as the hidden state of the recurrent network, \mathbf{r}_t , \mathbf{z}_t and \mathbf{n}_t as the network gates, \star as the term-by-term product, and \mathbf{W} . and \mathbf{b} . as the weights and bias respectively. One can show that applying e-prop in a classical GRU network is mathematically equivalent to applying BPTT in the network above.

In simulations, we evaluate the performance as the phoneme classification accuracy on the test set. We find that CLAPP achieves 61.7% with BPTT and 58.6% with e-prop; but the latter can be implemented with purely local learning rules by relying on eligibility traces [20]. In comparison, phoneme classification from the last feedforward layer before the RNN only yields 52.4% accuracy.

Table 5: Linear classification test accuracy (%) on STL-10 with features from a VGG-6 encoder trained with the CLAPP loss for different sizes of gradient-isolated modules. This data was used in the inset of Table 3.

# modules	# layers per module	Test accuracy (%)
6, i.e. layer-wise (CLAPP)	1	74.0
4 modules upper	3,1,1,1	75.4
4 modules lower	1,1,1,3	76.2
3 modules	2	77.4
2 modules	3	77.6
1 module (end-to-end) (see Table 1)	6	80.3

²<https://pytorch.org/docs/stable/generated/torch.nn.GRU.html>

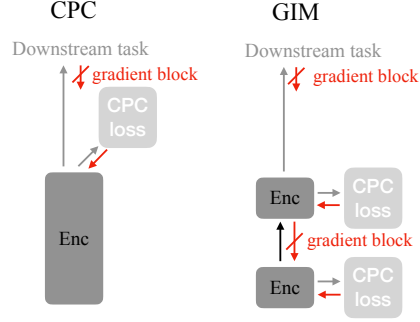


Figure 4: In Greedy InfoMax (GIM), the encoder network is split into several, gradient-isolated modules to which the CPC principle is applied separately. Gradient back-propagation is blocked between modules.

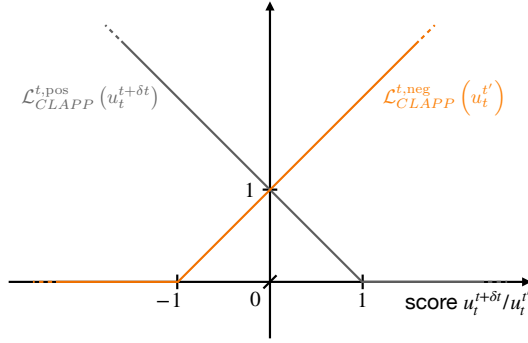


Figure 5: Illustration of the CLAPP loss, see Equation 2.

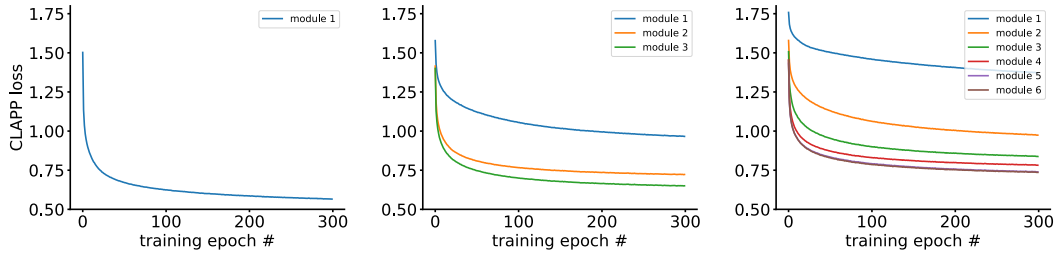


Figure 6: CLAPP training losses for encoders split into 1, 3 or 6 gradient-isolated modules.